Evolution of the electronic and geometric structure of size-selected Pt and Pd clusters on Ag(110) observed by photoemission

H.-V. Roy, P. Fayet,* F. Patthey, and W.-D. Schneider
Institut de Physique Expérimentale, Université de Lausanne, CH-1015 Lausanne, Switzerland

B. Delley
Paul-Scherrer-Institut, Badenstrasse 569, CH-8048 Zürich, Switzerland

C. Massobrio
Institut de Physique Expérimentale, Ecole Polytechnique Fédérale de Lausanne, CH-1015 Lausanne, Switzerland
(Received 22 March 1993; revised manuscript received 16 November 1993)

Mass-selected Pt_n and Pd_n ($n=1-15$) clusters, generated by ion bombardment, are deposited at room temperature in submonolayer quantities on an Ag(110) single-crystal surface and characterized by electron spectroscopy (x-ray-photoemission spectroscopy and ultraviolet photoemission spectroscopy). The monodispersed clusters indicate individual discrete electronic structure features of the Pt 5*d* and Pd 4*d* emission. For the monomers virtual bound-state formation as in dilute (3%) PtAg and PdAg alloys is observed. With increasing cluster size, first, the increasing splitting between the bondinglike and antibondinglike *d* states reflects the increase in cohesive energy due to molecular interaction and second, the shift of the center of gravity of the *d* emission towards the Fermi energy indicates the trend to metal formation. The Pt 4*f* and Pd 3*d* core levels show practically no shift with increasing cluster size indicating a two-dimensional cluster structure. Total-energy calculations, performed within this study using the embedded-atom method, suggest a chain structure for small Pt_n ($n=1-7$) and Pd_n ($n=1-17$) clusters on the Ag(110) surface, lying along the [$\bar{1}$10] direction.

I. INTRODUCTION

When atoms are brought together to form a solid, their outer wave functions overlap and the energy levels of the individual atoms broaden, becoming the energy bands of condensed matter. The observation of the evolution of this process from the single atom to the bulk as a function of the number of atoms involved would in principle give insight into the size dependence of many properties of condensed matter, for example the onset of metallic behavior,[1] or the raising of the melting temperature with cluster size.[2] If the clusters are supported on a substrate, their electronic and structural properties are expected to change by interaction with the substrate. Systematic studies of these changes as a function of cluster size may lead to a detailed understanding of, e.g., crystal growth or catalytic activity. This is important from both fundamental and technological points of view. With increasing miniaturization in microelectronics and optoelectronics, the physical properties of nanoscale structures determine the behavior of the devices. For example, the answer to the question of how many atoms of a metallic element are needed to obtain a cluster with metallic properties will be of primordial importance for the ultimate size of electrical contacts between nanostructures.

Up to now, most of experimental studies of the electronic structure of supported small particles were carried out on evaporated or sputtered materials when only some average particle size distribution could be achieved.[3-8] Only recently, photoemission data have been obtained from supported monosize mass-selected clusters.[9-11] In general, with decreasing particle size, shifts of core levels and valence bands as well as a narrowing of the valence bands are observed. In order to explain these findings, different models have been invoked, involving electronic structure changes in the ground state,[3] or in the photoemission final state.[5] For example, Wertheim concludes from available data that core-level shifts observed in supported metal clusters arise largely from the charge left on the cluster by electron emission. This point of view has been critized by Mason,[13] who favors initial-state changes being responsible for the shifts. On the other hand, Cini *et al.*[7] estimate initial-state energy shifts and cluster charging to play a minor role for the system Pd/C. They interprete the observed dependence of the spectra in terms of a mixing between substrate and cluster orbitals, where the coupling is proportional to the inverse cluster radius. However, recent experimental results on the same system (Pd/C) seem to confirm the cluster charge model of Wertheim.[5] One of the main reasons for this unclear situation has been mentioned by Mason.[13] "One of the problems with virtually all of the experimental work published is that there has been no real determination of the cluster sizes involved."

The geometric structure assumed by clusters on crystal planes reflects fundamental aspects of adatom-adatom and adatom-substrate interactions, e.g., it contains information about the initial stages of growth modes in epitaxy. For instance, the structure of Pt adatom clusters on Pt(100) is observed to oscillate between chain- and island-type configurations as the number of adatoms is increased from three to six.[14] Embedded-atom-method cal-

culations (EAM) are found to predict these results and show that lattice relaxations are a critical factor in covering this unusual series of structural transformations.[15]

In order to observe the detailed evolution of the electronic structure as a function of cluster size without the disturbing charge effect, we have chosen metal-on-metal systems. In the present study small mass-selected ($1 \leq n \leq 15$) transition-metal clusters (Pt, Pd) are deposited on a single-crystal Ag(110) substrate. These systems are of specific interest for the above-mentioned structural as well as electronic structure aspects. They represent dilute surface alloys with virtual bound-state formation,[16–19] giving insight into the microscopic adsorbate-substrate bonding mechanism.

The paper is organized as follows. In Sec. II experimental details of the cluster production and characterization by electron spectroscopic techniques is discussed. In Sec. III A the outer level photoemission spectra for supported monomers of Pt and Pd are shown and discussed, together with related dilute PtAg and PdAg alloys, within the single-impurity model of Anderson. Section III B presents the evolution of the electronic structure with cluster size for supported Pt and Pd clusters as observed in the outer level photoemission spectra. In Sec. III C structural information contained in the core-level binding-energy shifts of the adsorbed clusters is extracted and compared to predictions based on embedded-atom-method calculations, performed within this study. Finally, in Sec. IV, the results of this study are summarized, the open questions are addressed, and the directions of future work are indicated.

II. EXPERIMENTAL DETAILS

The experimental setup is shown in Fig. 1 and described in detail elsewhere.[11,12] Ionized clusters are produced by Xe-ion bombardment of Pt and Pd targets, mass selected by a quadrupole mass spectrometer and deposited at low kinetic energy (8±6 eV). The substrate, held at room temperature, is in the center of an UHV analysis chamber (2×10^{-10} mbar) allowing *in situ* characterization of the substrate and the supported clusters by low-energy electron diffraction (LEED) and photoemission [ultraviolet-photoemission spectroscopy (UPS) and x-ray photoemission spectroscopy (XPS)]. Coverages corresponding to 0.1 monolayer (ML) as determined by cluster beam current and deposition time have been prepared. Subsequently, photoemission measurements were carried out in a custom built VSW CLASS 150 electron spectrometer equipped with a Mg $K\alpha$ x-ray source and a high-intensity microwave gas-discharge lamp (GAMMADATA) producing photons of 21.2 eV (He I) and 40.8 eV (He II) energy. The vacuum ultraviolet (vuv) radiation is monochromatized by a homebuilt monochromator yielding satellite free photoelectron spectra. The instrumental resolution for XPS and UPS techniques was about 1.0 and 0.1 eV, respectively. The single-crystal Ag(110) surface was prepared by argon-ion bombardment and annealing. Within the detection limit of x-ray and ultraviolet photoemission the surface was found to be free of contaminants. Sharp low-energy electron-diffraction (LEED) spots indicated a well-ordered surface prior to adsorption. The deposition rates deduced from the cluster beam parameters correspond well to those obtained from Pt/Ag core-level intensity ratios.[20] Assuming statistically uncorrelated deposition on the Ag lattice and neglecting diffusion,[21] we calculate that at coverages of 0.02, 0.05, and 0.1 ML, respectively, 80%, 60%, and 32% of the incoming monomers have survived as single atoms (and not as dimers, trimers, etc.) after deposition, in agreement with recent estimates.[22] Taking into account the geometry of the Ag(110) surface, where the troughs are oriented along the [$\bar{1}$10] direction, we can restrict the above consideration to a maximal two neighbors within the [$\bar{1}$10] channels. Then after deposition of 0.05 and 0.1 ML, 87% and 74%, respectively, of the incoming atoms survive as monomers. With increasing cluster size the same ($\sim$0.1 ML) total surface-atom con-

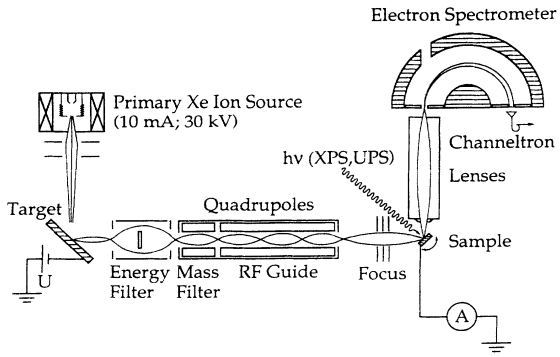

FIG. 1. Scheme of the experimental setup for the production, size selection, deposition, and *in situ* characterization of mass-selected clusters.

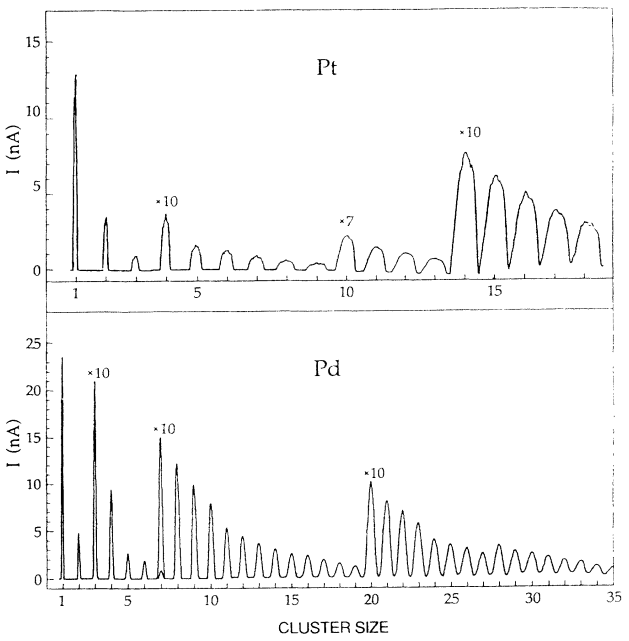

FIG. 2. Mass spectra of positively charged platinum and palladium clusters.

centration is maintained, so that any changes in the photoemission spectra are due to cluster-size effects and not to a changing surface-atom concentration.

The mass spectra of positively charged clusters from Pt_1^+ to Pt_{18}^+, and of Pd_1^+ to Pd_{34}^+ measured at relatively high resolution, are shown in Fig. 2. The increase of the peak width in the Pt spectrum reflects the isotope configuration of natural platinum. At higher transmission the measured intensities can reach 80 nA. These experimental facts clearly show the ability to obtain sufficient cluster beam currents to perform the deposition of mass-selected clusters in the range of small particle sizes. Typical deposition data for Pt clusters are given elsewhere.[23]

III. RESULTS AND DISCUSSION

A. Supported monomers: Electronic structure Pt_1/Ag(110) and Pd_1/Ag(110) versus dilute PtAg and PdAg alloys

Figure 3 displays the outer level photoelectron spectra, excited with He I radiation and measured at normal emission, of (a) the clean Ag(110) surface, (b) at 0.1-ML Pt coverage, and (c) at 0.1-ML Pd coverage. The spectrum of clean Ag(110) is in excellent agreement with the literature.[24] We note that, owing to the present experimental setup, no additional intensity due to a He I satellite is present in the flat Ag *sp* part of the spectrum. The spectrum in Fig. 3(b) shows two small peaks at 1.6- and 2.6-eV binding energy (amplified by a factor of 10 in the inset) which are due to Pt 5*d* emission from the adsorbed dilute Pt atoms. The identification of the two structures is rather straightforward when compared with photoemission results on dilute PtAg alloys.[25–27] They are attributed to emission from atomiclike Pt $5d_{5/2,3/2}$ states with an experimentally derived spin-orbit splitting of 1.0±0.05 eV, in excellent agreement with the gas phase value for the Pt $5d^9$ configuration.[28] This interpretation suggests that the Pt-substrate interaction changes the atomic $5d^9 6s^1$ configuration to $5d^{10-x}s^x (0<x<1)$. For Pd monomers a similar behavior is observed [Fig. 3(c)], where now the spin-orbit splitting of the Pd 4*d* states amounts to 0.35±0.05 eV, again in excellent agreement with the gas-phase value for the Pd $4d^9$ configuration.[28] The striking observation in the Pt data is that the Pt $5d_{5/2}$ component appears to have a linewidth twice as large as the Pt $5d_{3/2}$ component. Calculations performed within the Anderson single-impurity model clearly suggest that this effect is mainly caused by an energy-dependent coupling between the Pt 5*d* state and the Ag conduction-band state.[29] The hybridization broadens the sharp atomic level into a resonance state (virtual bound state) and induces a ground-state occupation for the Pt 5*d* shell of $n_d=9.88$. Considering the Pt $5d^{10-x}6s^x$ configuration discussed above, this result fixes quantitatively $x=0.12$ as a consequence of the adsorbate-substrate interaction.

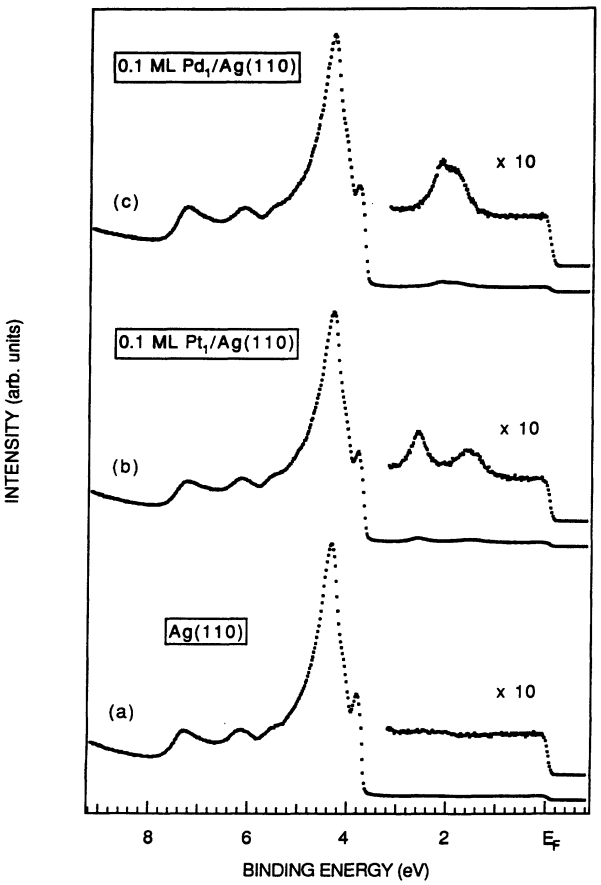

FIG. 3. Outer-level photoemission spectra of (a) clean, (b) Pt-covered (0.1 ML), and (c) Pd-covered (0.1 ML) Ag(110) surfaces taken at 21.2-eV photon energy.

Similar calculations were performed for the spectra of Pd_1/Ag(110) and dilute alloys PtAg and PdAg.[30] In the former case, the simulation is satisfactory using the same hybridization function as for Pt_1/Ag(110). For the alloys, however, the strength of the hybridization had to be increased by factors of 2.6 and 1.8, respectively, in order to achieve agreement with experiment. Starting from the natural hypothesis that the hybridization should be proportional to the overlap of the outer wave functions, to a first approximation it should be proportional to the number of nearest Ag atoms. At the surface an impurity has five neighbors, in the dilute alloys (fcc) there are 12, i.e., the hybridization should increase by a factor of 2.4 in the alloy. These differences between Pt and Pd alloys point to the fact that the detailed overlap of the wave functions has to be considered in addition to the simple coordination number argument.

With increasing hybridization the *d* occupation n_d decreases so that in going from the adsorbed Pt (Pd) impurity to the dilute alloy impurity we obtain a change in n_d from 9.88 (9.89) to 9.74 (9.80). This trend is in agreement with theoretical expectations where Pt (Pd) metal has a *d* occupation of 9.06 (9.41) electrons.[31]

B. Supported clusters: Electronic properties of Pt_n/Ag(110) and Pd_n/Ag(110) outer level spectra

Figures 4 and 5 display the transition-metal *d* contribution from small clusters of Pt and Pd to the excitation spectra in an energy range between the Fermi energy and

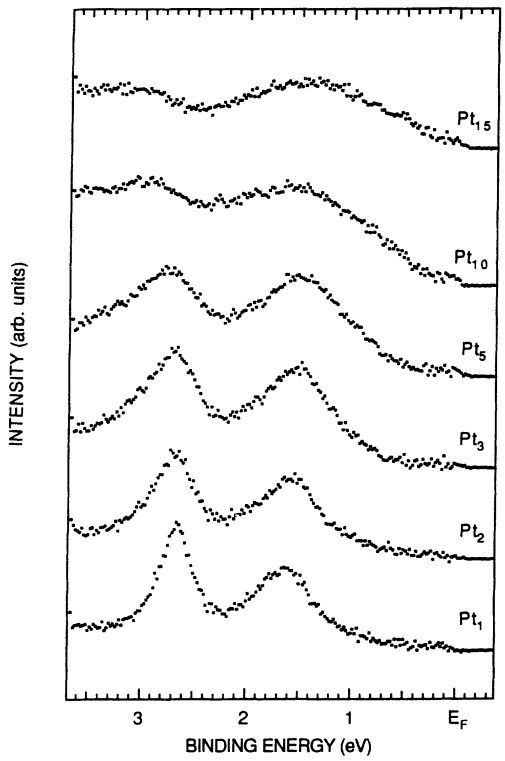

FIG. 4. Evolution of the Pt 5*d* emission as a function of cluster size. These spectra are difference spectra between Pt-covered and clean Ag spectra (see Fig. 3).

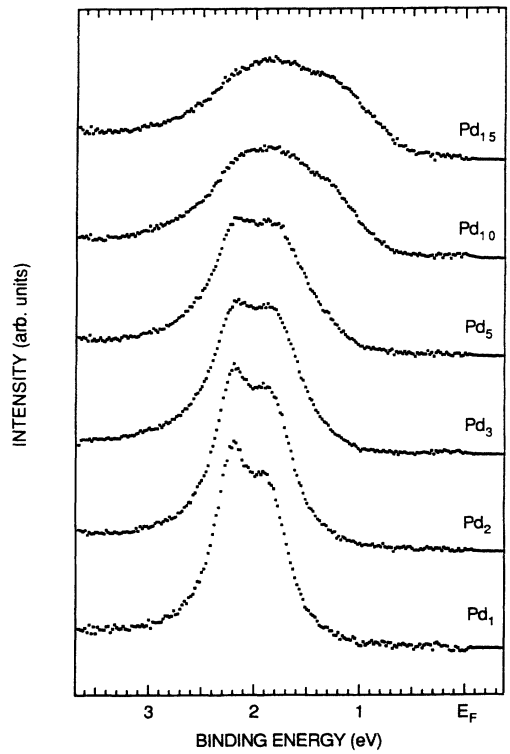

FIG. 5. Evolution of the Pd 4*d* emission as a function of cluster size. These spectra are difference spectra between Pd-covered and clean Ag spectra (see Fig. 3).

3.6-eV binding energy for the cluster sizes indicated. These difference spectra are obtained by subtracting the pure Ag(110) spectrum, normalized at the top of the *sp* band just below the Fermi level, from the total spectra. For Pt clusters the following general trend is observed: the two prominent structures observed in the atomic limit broaden and shift in energy in opposite directions. This observation seems to favor an interpretation of the size-dependent evolution of the electronic structure in terms of bondinglike and antibondinglike *d* states, reflecting the increase in cohesive energy due to molecular interaction. Moreover there is a continuous weight transfer toward the lower binding-energy component leading to a shift of the center of gravity of Pt 5*d* emission toward the Fermi energy with increasing cluster size. The same trend but less pronounced is found for the Pd clusters. We note that these observations confirm earlier results on non-size-selected Pd and Pt clusters obtained by evaporation on Xe films condensed on metallic samples.[6,32]

In Fig. 6(a) we have plotted this shift of the center of gravity of the *d* emission as a function of cluster size. For Pt cluster sizes larger than 5 a slight discontinuity of the general trend is observed. This is due to the fact that the higher-lying 5*d* binding-energy component starts to overlap with the Ag 4*d* emission and, therefore, the Pt 5*d* contribution is underestimated in this energy range. Figure 6(b) displays the cluster-size-dependent widths of the total *d* emission, which should reflect the Pt-Pt and Pd-Pd interaction. In view of the position of density of states of pure Pt and Pd metal[25] with respect to E_F, the shift of the center of gravity of the *d* states toward the Fermi level and their concomittant broadening clearly indicate the trend to transition-metal formation already at such small cluster sizes.

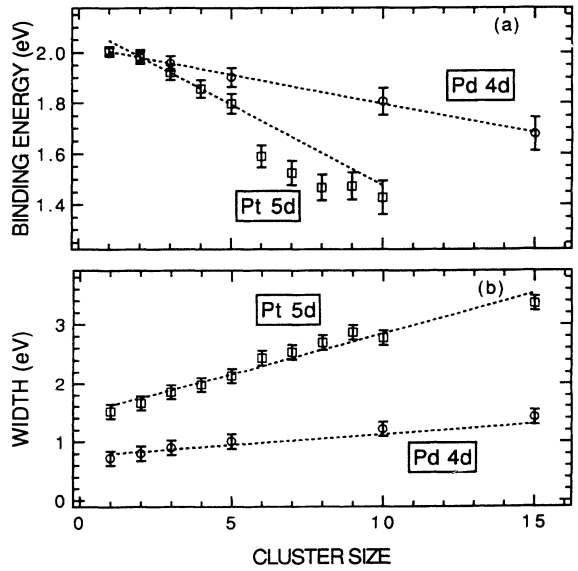

FIG. 6. (a) Shift of the center of gravity for the Pd 4*d* and Pt 5*d* emission as a function of cluster size. (b) Evolution of the total width of the Pt 5*d* and Pd 4*d* valence level emission as a function of cluster size. The dotted lines are drawn to guide the eye.

C. Supported clusters: Structural properties

1. *Core-level analysis: Binding energies and linewidths*

Structural information of the supported clusters is contained in the core-level binding energies. It is known that core-level binding energies undergo characteristic changes at surfaces due to the reduced coordination as compared to the bulk.[33] The analysis of this so-called surface core-level shift (SCS) has been useful, e.g., for structural analysis on single crystal surfaces. For Ir and Au different orientations of the surfaces could be discriminated, and surface reconstruction could be discerned.[34,35] Even on amorphous surfaces of cold condensed Yb films an identification of multiple surface shifts in terms of different coordination numbers of surface atoms was possible.[36] In order to extract structural information from our Pt and Pd core-level data as a function of cluster size, the Pt $4f_{7/2}$ and Pd $3d_{5/2}$ core levels have been analyzed by a least-squares-fit procedure.[37] The data were best fitted by a set of Doniach-Sunjic line shapes[38] convoluted with a Gaussian of 1.0 eV full width at half maximum (FWHM) representing the overall resolution of the experiment (x-ray linewidth and spectrometer resolution). The observed asymmetry[39] (α is between 0.05 and 0.1) points to metallic screening of the Pt and Pd core holes by Ag conduction electrons. Figure 7 shows the result of this analysis for the Pt $4f_{7/2,5/2}$ and Pd $3d_{5/2}$ core levels of the monomers.

Figure 8 shows the evolution of the Pt and Pd linewidths with cluster size. The values for the pure metals are also indicated.[40] For Pt clusters we note that with increasing cluster size the linewidth increases and then levels off for clusters containing more than six atoms. The observation is in contrast to earlier results of small Pt clusters on SiO_2 substrates.[10] Moreover the linewidth in the present case of a single-crystal substrate is much smaller (less than 0.5 eV), than for the Pt/SiO_2 system (between 1.4 and 1.8 eV) and for the Pt/Ag film system (1.3 eV) at 110 K substrate temperature.[41] These observations seem to indicate that most of the linewidth contributions for rough surfaces, in addition to phonon broadening, are due to inequivalent lattice sites of the cluster adatoms on the support. On the other hand, the increasing linewidth for the Pt clusters is probably due to the increasing number of Pt neighbors. For Pd clusters this effect is practically absent. A possible reason for this behavior will be given below.

Figure 9 displays the evolution of the measured core-level binding energies with cluster size. For comparison the corresponding bulk value for the respective core level as well as for the dilute alloys are also indicated. For Pt, in contrast to metal-on-graphite and metal-on-insulator/semiconductor systems, the core-level binding energy is found to be at lower binding energy than the bulk value. In principle, in order to evaluate core-level binding-energy shifts, the energy between the core-level binding energy of Pt or Pd in bulk Ag has to be compared with the corresponding values at the surface.[3,33] In the present case, as shown in Fig. 9, these values are identical within the error bars. It is gratifying to note that the measured and calculated core-level binding energy shifts in dilute alloys of PtCu and PtAu, electronically similar to the present system, show also a negative shift with respect to the binding energy of the core level of pure Pt.[42] On the other hand, the core-level binding energies found for the dilute PdAg system and for

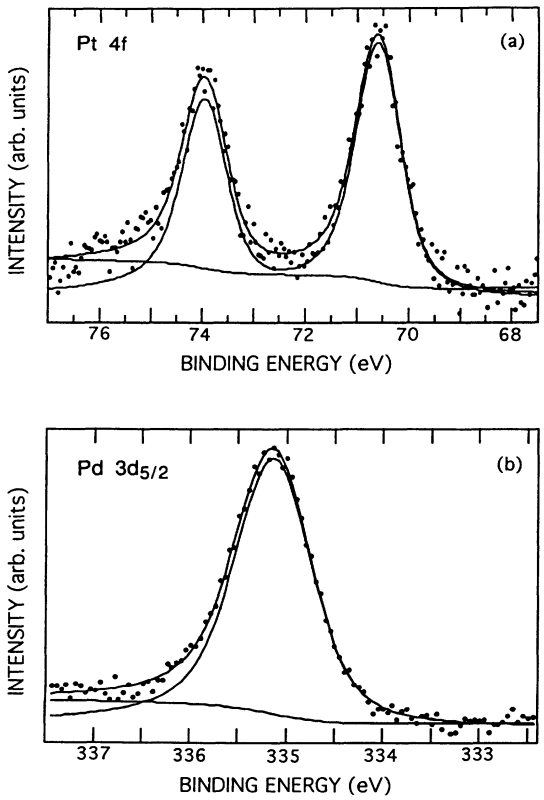

FIG. 7. (a) Pt $4f$ core-level spectrum and line-shape analysis (see text) for 0.1-ML Pt monomers on Ag(110). (b) Pd $3d_{5/2}$ core-level spectrum and line-shape analysis for 0.1-ML Pd monomers on Ag(110).

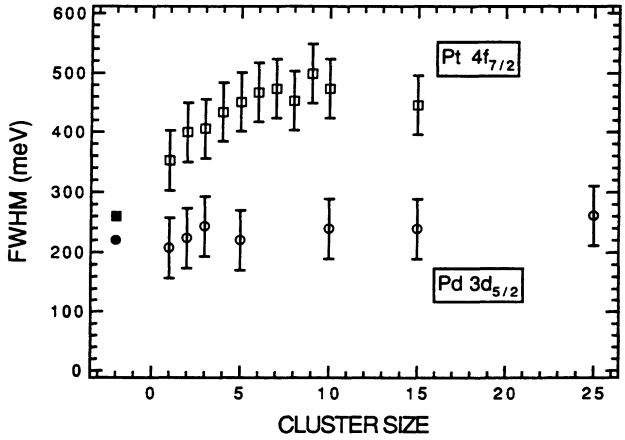

FIG. 8. Evolution of the core-level linewidth (FWHM) with cluster size. The values for the pure metals Pt (filled square) and Pd (filled circle) are indicated.

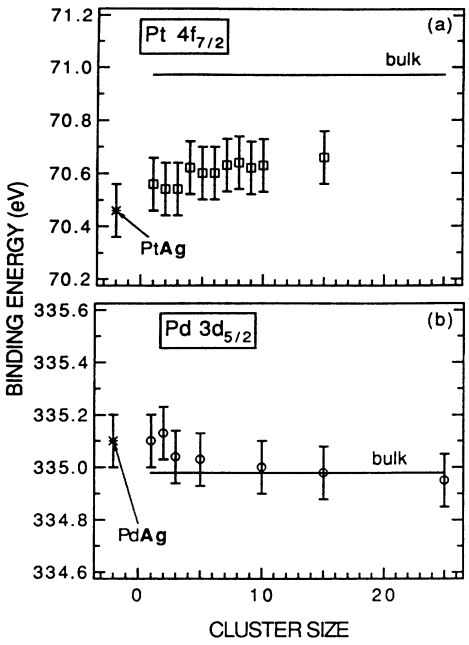

FIG. 9. Evolution of the core-level binding energies, taken from an analysis as shown in Fig. 7, as a function of cluster size. For comparison the values for the bulk (horizontal lines) and dilute metals (asterix) are also given.

Pd_1/Ag(110) show a slight trend to positive binding-energy shift, which is at most 0.1 eV, whereas in an earlier study of this alloy system (formed by coevaporation) values of 0.5 eV have been determined.[42] With increasing cluster size the bulk value is reached very quickly.

These shifts should be calculable from a first-principles calculation.[43] However, we can draw some conclusions from the measured core-level binding-energy positions. Measured surface shifts for Pt(100) ($4f_{7/2}=70.7$ eV),[44] Pt(111) ($4f_{7/2}=70.5$ eV),[45] and Pd(110) ($3d_{5/2}$) (Ref. 46) are -0.4 eV. As shown for Pt in Fig. 9(a) the core-level binding energy approaches gradually the surface value with increasing cluster size. If the clusters would form three-dimensional (3D) islands we should also expect typical bulk core-level binding energies around 71 eV. The different behavior of Pt and Pd core-level linewidths and binding energies as manifested in Figs. 8 and 9 might be due to the presence of hydrogen originating from the cluster source, reducing strongly the intensity of the Pd surface peak.[46]

From the behavior of the Pt $4f$ and Pd $3d$ binding energy with cluster size (within the experimental resolution of our experiment), it is suggested that these small clusters form chains and/or two-dimensional islands, in agreement with recent findings for Pb/Ag.[47] Moreover, field ion microscopy experiments of related metal-on-metal systems (Pt/Pt, Pd/Pt) together with embedded-atom calculations[14,15] support this view of one- and two-dimensional adcluster structures. In order to obtain a consistent picture within our adsorbate-substrate system Pt/Ag(110) and Pd/Ag(110), we performed embedded-atom-method calculations within the present study, as described in more detail below.

2. *Embedded-atom-metal calculations: Binding energies and proposed adclusters structures*

Embedded-atom-method (EAM) calculations[48] represent a powerful atomistic tool to determine the energetics and dynamics of transition-metal systems, as proved by a large number of results for bulk and surface properties consistent with experimental findings.[49–52] Recent convincing examples of application of the EAM scheme to the determination of the most stable structures in the case of Pt and Pd clusters on the Pt(001) surface[14,15] motivate the use of such an approach to obtain relevant information on structural features for Pt and Pd clusters on Ag(110). Our main concern here is to predict the most stable structures of the adsorbed clusters through the computation of their binding energy, thereby providing a self-contained microscopic-scale picture of the way they are adsorbed on the surface. Furthermore, the comparison with structural information extracted from photoemission data is extremely useful to judge on the reliability of the EAM method to describe physical situations not included in the construction of the potentials, which are typically fitted to bulk data only.

The interatomic potentials developed by Foiles, Baskes, and Daw[48] are based on an expression of the total energy of the system as the energy required to embed a given atom into the electron density provided by the remaining atoms plus a core-core repulsion potential which has the form of a pair potential. The potential energy is written

$$E_{\text{pot}}=\sum_i F_i(\rho_i)+\sum_i\sum_{j\neq i}\Phi(r_{ij})$$
$$=\sum_i F_i\left[\sum_{j\neq i}\rho_{ja}(r_{ij})\right]+\sum_i\sum_{j\neq i}\Phi(r_{ij})\ . \quad (1)$$

In (1) F_i is the embedding energy of atom i, r_i is the electron density at atom i, and $\Phi(r_{ij})$ the repulsive interaction between pairs of atoms separated by a distance r_{ij}. The electron densities ρ_i pertaining to each atom are approximated with the superposition of the atomic electron densities ρ_{ja} from the other atoms. The practical details of the fitting procedure leading to the complete determination of the embedding energies and pair interactions have been largely detailed in the literature and need not be discussed here.

In our computations were employed a slab of 4608 Ag atoms arranged in a parellelepipedic box with X, Y, and Z directions along the [001], [$\bar{1}$10], and [110] crystallographic axes, respectively, with periodic boundary conditions applied only in the X and Y directions. The interatomic potentials are continuous at a cutoff distance R_c equal to 5.25 Å. We choose edge lengths $L_x=18a\sqrt{2}$, $L_y=16a$, and $L_Z=4a/\sqrt{2}$, with a equal to the lattice parameter, each XY plane containing 576 atoms. The interplanar distance along the Z direction is $d_p=a/(2\sqrt{2})$. The total energy of a given adsorbate/substrate system is obtained by positioning the N cluster atoms above the uppermost Ag(110) plane in adsorption sites corresponding to linear, compact or three-dimensional geometrical arrangements, as displayed in Fig. 10 for $N=8$. Atoms in

one- and two-dimensional structures are initially set at a distance d_p above the uppermost Ag(110) plane, the most stable two-dimensional structures being made of two identical linear chains lying along the $[\bar{1}10]$ direction and separated by a along the [001] direction. In three-dimensional structures, studied for $N=5$, 8, 11, 14, and 17, $N'=(N-2)/3$ adatoms are initially placed at a distance $2d_p$ above the uppermost (110) layer and, on the XY plane, in between two rows made of $(N+1)/3$ atoms arranged as in the two-dimensional case. The minimum of the energy is then searched for by using a quenched molecular-dynamics minimization technique.[53] In the following our results, referring to energies and configurations obtained upon relaxation, will be presented in terms of binding energies E_b defined as $E_b=(E_N-E_{\text{slab}})-N(E_1-E_{\text{slab}})$, where E_N is the total energy of the system with N adsorbed atoms, and E_{slab} is the total energy of the Ag(110) slab with two adatoms.

As shown in Fig. 11, linear chains are always preferred

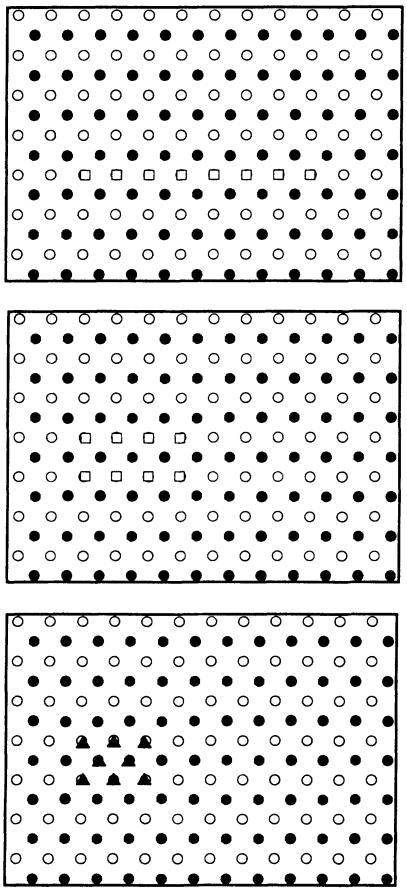

FIG. 10. Top views of the (110) plane showing the two uppermost substrate layers (open and full circles, with the full circles representing the highest plane along the [110] direction) and the clusters adsorbed at the top upon relaxation. From top to bottom, for an adsorbed cluster of eight atoms: a linear-chain (open squares) two-dimensional structure with two rows of four atoms along the $[\bar{1}10]$ directions (open squares), and a three-dimensional structure (full triangles) with two inner atoms higher along the $[\bar{1}10]$ direction.

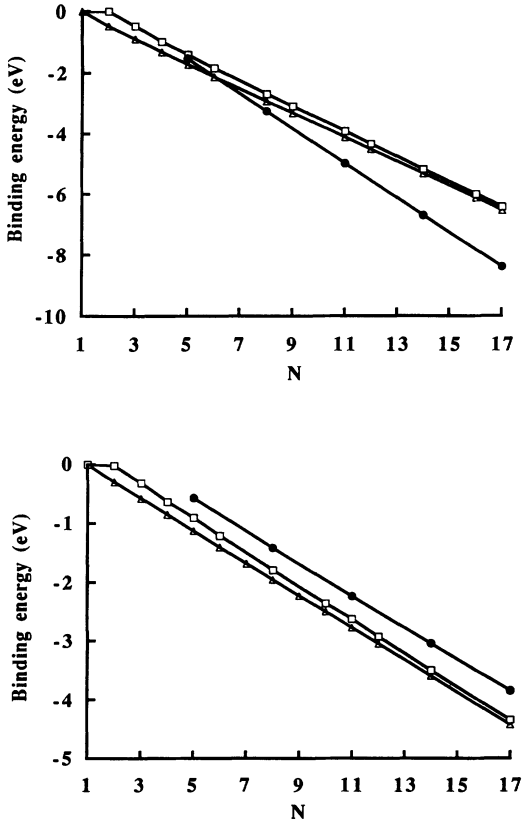

FIG. 11. Binding energies for adsorbed Pt (upper part) and Pd (lower part) clusters on Ag(110). Full circles, three-dimensional structures; open squares, two-dimensional structures, open triangles, linear chains.

to two-dimensional islands for both Pt/Ag(110) and Pd/Ag(110), at least up to the largest sizes of clusters ($N=17$) we considered. The observation of the geometry of one- and two-dimensional structures on the (110) surface indicates that a simple bond-counting argument applies in this case, since linear chains are characterized by a larger number of strong nearest-neighbor interactions along the $[\bar{1}10]$ direction ($N-1$ against $N-2$), and the number of nearest neighbors of different kinds is the same in the two situations. More intriguing is the trend displayed by three-dimensional structures, which are definitely higher in energy for Pd/Ag(110) but lower for $N\geq 8$ in the case of Pt/Ag(110). Since three-dimensional structures have a smaller number of nearest-neighbor interactions with the substrate, but a larger number of interactions among constituent atoms, it is expected that the strength of the Ag-Pd(Pt), and Pd(Pt)-Pd(Pt) interactions at the topmost layer level will play a crucial role in determining the relative stability of the two arrangements. To elucidate this point, we derived from the N-body interatomic potential given in (1) environment-dependent effective pair potentials[54] which take the form

$$\psi_{ij}(r_{ij})=F_i'(\rho_i)\rho_{ja}(r_{ij})+F_j'(\rho_j)\rho_{ia}(r_{ij})+\Phi_{ij}(r_{ij})\ . \qquad (2)$$

These quantities allow us to estimate the strength of the interaction for a given pair of atoms, and are represented in Fig. 12 for both systems Pd/Ag(110) and

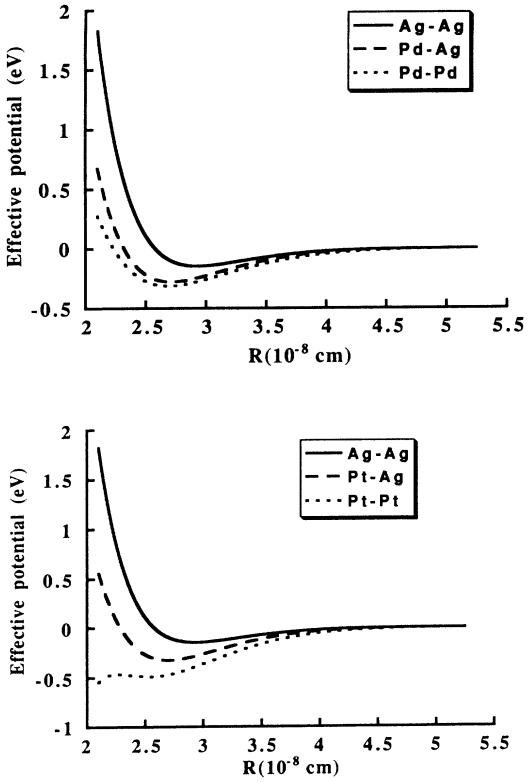

FIG. 12. Upper part: Effective two-body potentials for Ag and Pd relative to the Ag-Pd, Ag-Ag, and Pd-Pd interactions at the uppermost Ag(110) plane level. Lower part: the same for the Pt-Ag system.

Pt/Ag(110). The effective potentials are those relative to the Pt (or Pd) adatom closer to the surface along the [110] direction, and to one of its Ag nearest neighbors of the substrate.

The origins of the stability of one-dimensional linear chains in Pd/Ag(110) and three-dimensional structures in Pt/Ag(110), predicted within the EAM scheme, can easily be understood by considering the number of first neighbors of a given kind (N^L_{A-B} for linear chains and N^{3d}_{A-B} for three-dimensional structures), and the values $\psi_{ij}(R^L_{A-B})$ and $\psi_{ij}(R^{3d}_{A-B})$ taken by $\psi_{ij}(r_{ij})$ at the average bond distances R^L_{A-B} and R^{3d}_{A-B}, where in the above definitions the indicates A and B stand for Pt/Pt, Pt/Ag, Pd/Pd, and Pd/Ag interactions. As an example, we collect in Table I the resulting stabilization energies E^{3d}_{Pt}, E^L_{Pt}, E^{3d}_{Pd}, and E^L_{Pd} for $N=8$, given by the sums of the products $N^{3d}_{Pt\text{-}Pt}\psi_{ij}(R^{3d}_{Pt\text{-}Pt})$, $N^{3d}_{Pt\text{-}Ag}\psi_{ij}(R^{3d}_{Pt\text{-}Ag})$ and $N^L_{Pt\text{-}Pt}\psi_{ij}(R^L_{Pt\text{-}Pt})$, $N^L_{Pt\text{-}Ag}\psi_{ij}(R^L_{Pt\text{-}Ag})$ with similar expressions holding in the Pd/Ag case. From Table I and Fig. 12 it can be deduced that strong Pt-Pt interactions are indeed responsible for the enhanced stability of Pt three-dimensional structures on Ag(110). In fact, in the case of Pd/Ag, the effective Pd/Pd interatomic potential lies very close to the Ag/Pd one, thereby making the linear structure more stable as a simple consequence of a larger total number of first-neighbor bonds (47 against 45 in the three-dimensional case for $N=8$). On the other hand the

TABLE I. Number of nearest neighbors N^L_{A-B} and N^{3d}_{A-B}, averaged nearest-neighbor bond distances R^L_{A-B} and R^{3d}_{A-B}, corresponding values of the effective two-body potentials $\psi_{ij}(R^L_{A-B})$ and $\psi_{ij}(R^{3d}_{A-B})$ and stabilization energies E^{3d}_{Pt}, E^L_{Pt}, E^{3d}_{Pd}, and E^L_{Pd} for Pt and Pd clusters of eight atoms adsorbed on Ag(110).

	Pt/Ag(110)	Pd/Ag(110)
N^L_{A-B}	40	40
N^L_{B-B}	7	7
N^{3d}_{A-B}	32	32
N^{3d}_{B-B}	13	13
R^L_{A-B} (10^{-8} cm)	2.658	2.684
R^L_{B-B} (10^{-8} cm)	2.803	2.850
R^{3d}_{A-B} (10^{-8} cm)	2.706	2.709
R^{3d}_{B-B} (10^{-8} cm)	2.631	2.706
$\psi_{ij}(R^L_{A-B})$ (eV)	−0.324	−0.277
$\psi_{ij}(R^L_{B-B})$ (eV)	−0.479	−0.295
$\psi_{ij}(R^{3d}_{A-B})$ (eV)	−0.326	−0.267
$\psi_{ij}(R^{3d}_{B-B})$ (eV)	−0.484	−0.296
E^{3d} (eV)	−16.724	−12.392
E^L (eV)	−16.316	−13.145

Pt-Pt interaction becomes strongly attractive at very short distances for low coordination numbers, resulting in a contribution to the cohesive energy which is predominant over the one due to Ag-Pt interactions. The above results indicate that EAM predictions for adsorbed clusters with up to $N=17$ atoms point toward the stability of one-dimensional linear chains for Pd on Ag(110), while in the case of Pt/Ag(110) three-dimensional structures, less stable than one dimension for $N=5$, become increasingly more stable for $N=8$, 11, and 17. The trends of Fig. 11 suggest that in both cases two-dimensional structures made of two parallel chains along the [$\bar{1}$10] direction are expected to become lower in energy than one-dimensional ones beginning from a cluster size $N=25$. However, the peculiar shape of the Pt-Pt effective interactions for atoms in the cluster, especially when compared to the well-behaved shape of the Pd-Pd interaction, raises a question about the reliability of the EAM modeling of Pt, at least in the form of Ref. 48, especially for low coordinated atoms.

In view of these considerations we find the agreement on the Pd/Ag(110) structures between EAM and photoemission data predictions quite satisfactory, while the different results obtained in the Pt/Ag(110) case should stimulate further experimental and theoretical work to understand the origins of the discrepancy. In particular, on the simulation side, we intend to simulate experimental conditions more closely by considering the temperature-dependent behavior of a distribution of clusters of a given size for a given fraction of adsorbed monolayer.

IV. SUMMARY AND OUTLOOK

This work has shown the feasibility of preparing supported metal clusters with individually selected cluster sizes, and their *in situ* characterization by electron spec-

troscopies. For Pt and Pd monomers the formation of virtual bound states has been observed, and has been simulated successfully by many-body calculations within the Anderson single-impurity model. The evolution of the outer level spectra as a function of cluster size has been followed experimentally, and some qualitative features concerning bonding and the trend toward metal formation could be derived. Here clearly more theoretical work is necessary, for example Anderson-type calculations with several impurities or molecular-dynamics-type calculations. The structural information contained in the core-level binding energies has been used to predict one- or two-dimensional cluster structures at the Ag(110) surface. Total-energy calculations, performed within this study using the embedded-atom method, indeed suggest a chain structure for small Pt and Pd clusters on this surface, lying along the Ag[$\bar{1}$10] direction. The final proof for the reality of the one-dimensional structure adopted by these metal-on-metal systems has to come from scanning tunneling microscopy.[55] Experiments to clarify these structural aspects and to complement the spectroscopic information obtained so far are planned in the near future.

ACKNOWLEDGMENTS

The authors would like to thank O. Gunnarsson, E. Bullock, R. Berndt, and P. Feschotte for stimulating discussions; T. Detzel, J. Boschung, and J.-F. Jeanneret for their help during some of the experiments; and the Swiss National Science Foundation for financial support.

*Present address: Tetra Pak Romont SA, CH-1680 Romont, Switzerland.

[1]E. Schumacher, F. Blatter, M. Frey, U. Heiz, U. Röthlisberger, M. Schär, A. Vayloyan, and Ch. Yeretzian, Chimia **42**, 357 (1988).

[2]Ph. Buffat and J.-P. Borel, Phys. Rev. A **13**, 2287 (1976).

[3]M. G. Mason, Phys. Rev. B **27**, 748 (1983).

[4]S. B. DiCenzo and G. K. Wertheim, Comments Solid State Phys. **11**, 203 (1985).

[5]G. K. Wertheim, Z. Phys. D **12**, 319 (1989).

[6]S. Raaen and M. Strongin, Phys. Rev. B **32**, 4289 (1985).

[7]M. Cini, M. De Crescenzi, F. Patella, N. Motta, M. Sastry, F. Rochet, R. Pasquali, A. Balzarotti, and C. Verdozzi, Phys. Rev. B **41**, 5685 (1990).

[8]Ch. Kuhrt and M. Harsdorff, Surf. Sci. **245**, 173 (1991).

[9]S. B. DiCenzo, S. D. Berry, and H. E. Hartford, Jr., Phys. Rev. B **38**, 8465 (1988).

[10]W. Eberhardt, P. Fayet, D. M. Cox, Z. Fu, Z. Kaldor, R. Sherwood, and D. Sondericker, Phys. Rev. Lett. **64**, 780 (1990).

[11]P. Fayet, F. Patthey, H.-V. Roy, Th. Detzel, and W.-D. Schneider, Surf. Sci. **269/270**, 1101 (1992).

[12]H.-V. Roy, P. Fayet, F. Patthey, and W. D. Schneider, in *Cluster Models for Surface and Bulk Phenomena,* edited by G. Pacchioni, P. S. Bagus, and F. Parmigiani, *NATO Advanced Study Institute Series B: Physics,* Vol. 283 (Plenum, New York, 1992), p. 177.

[13]M. G. Mason, in *Cluster Models for Surface and Bulk Phenomena,* edited by G. Pacchioni, P. S. Bagus, and F. Parmigiani, *NATO Advanced Study Institute Series B: Physics,* Vol. 283 (Plenum, New York, 1992), p. 115.

[14]P. R. Schwoebel, S. M. Foiles, C. L. Bisson, and G. L. Kellogg, Phys. Rev. B **40**, 10 639 (1989).

[15]A. F. Wright, M. S. Daw, and C. Y. Fong, Phys. Rev. B **42**, 9409 (1990).

[16]J. Friedel, Nuovo Cimento Suppl. **7**, 287 (1958).

[17]P. W. Anderson, Phys. Rev. **124**, 41 (1961).

[18]J. W. Gadzuk, Surf. Sci. **43**, 44 (1974).

[19]G. C. Smith, C. Norris, C. Binns, and H. A. Padmore, J. Phys. C **15**, 6481 (1982).

[20]S. M. Goldberg, C. S. Fadley, and S. Kono, J. Electron Spectrosc. Relat. Phenon. **21**, 285 (1981).

[21]A recent experimental study (thermal energy atom scattering) of Pt/Cu(110) indicates that the adatoms do not diffuse up to 330 K. M. B. Hugenschmidt and C. de Beauvais, Surf. Sci. (to be published).

[22]D. M. Cox, B. Kessler, P. Fayet, E. Eberhardt, R. D. Sherwood, and A. Kaldor, in *Clusters and Cluster-Assembled Materials,* edited by R. S. Averback, J. Gernhole, and D. L. Nelson, MRS Symposium Proceedings No. 206 (Materials Research Society, Pittsburgh, 1991), p. 351.

[23]H.-V. Roy, J. Boschung, P. Fayet, F. Patthey, and W.-D. Schneider, Z. Phys. D **26**, 252 (1993).

[24]H. F. Roloff and H. Neddermeyer, Solid State Commun. **21**, 561 (1977).

[25]S. Hüfner, in *Photoemission in Solids,* edited by L. Ley and M. Cardona, Topics in Applied Physics Vol. 27 (Springer, Berlin, 1979), p. 173.

[26]D. van der Marel, G. A. Sawatzky, and J. A. Julianus, J. Phys. F **14**, 281 (1984).

[27]D. van der Marel, J. A. Julianus, and G. A. Sawatzky, Phys. Rev. B **32**, 6331 (1985).

[28]A. A. Radzig and B. M. Smirnov, *Reference Data on Atoms, Molecules and Ions* (Springer, Berlin, 1985).

[29]H.-V. Roy, J. Boschung, P. Fayet, F. Patthey, W.-D. Schneider, and B. Delley, Phys. Rev. Lett. **70**, 2653 (1993).

[30]H.-V. Roy, F. Patthey, W. D. Schneider, and B. Delley (unpublished).

[31]W. A. Harrison, *Electronic Structure and the Properties of Solids* (Freeman, San Francisco, 1980), p. 498.

[32]J. Colbert, A. Zangwill, M. Strongin, and S. Krummacher, Phys. Rev. B **27**, 1378 (1983).

[33]B. Johansson and N. Mårtensson, Phys. Rev. B **21**, 4427 (1980).

[34]J. F. van der Veen, F. J. Himpsel, and D. E. Eastman, Phys. Rev. Lett. **44**, 189 (1980).

[35]P. Heimann, J. F. van der Veen, and D. E. Eastman, Solid State Commun. **38**, 595 (1981).

[36]W.-D. Schneider, C. Laubschat, and B. Reihl, Phys. Rev. B **27**, 6538 (1983).

[37]P. H. Mahowald, D. J. Friedman, G. P. Carey, K. A. Bertness, and J. J. Yeh, J. Vac. Sci. Technol. A **5**, 2982 (1987).

[38]S. Doniach and M. Sunjic, J. Phys. C **3**, 2875 (1970).
[39]P. H. Citrin, G. K. Wertheim, and Y. Baer, Phys. Rev. B **27**, 3160 (1983).
[40]G. K. Wertheim and P. H. Citrin, in *Photoemission in Solids,* edited by M. Cardona and L. Ley, Topics in Applied Physics Vol. 26 (Springer, Berlin, 1979), p. 173.
[41]H.-V. Roy, P. Fayet, F. Patthey, and W. D. Schneider (unpublished).
[42]P. Steiner, S. Hüfner, H. Mårtensson, and B. Johansson, Solid State Commun. **37**, 73 (1981).
[43]M. Methfessel, D. Hennig, and M. Scheffler, Surf. Sci. **287/288**, 785 (1993); M. Aldén, H. L. Skiver, and B. Johansson, Phys. Rev. Lett. **71**, 2449 (1993).
[44]N. Barrett, C. Guillot, J. C. Bertolini, J. Messardier, and B. C. Khanra, Surf. Sci. Lett. **260**, L11 (1992).
[45]O. Björnholm, A. Nilsson, H. Tillborg, P. Bennich, A. Sandell, B. Hernnäs, C. Puglia, and N. Mårtensson (unpublished).
[46]R. Nyholm, M. Qverford, J. N. Anderson, S. L. Sorensen, and C. Wigren, J. Phys. Condens. Matter **4**, 277 (1992).
[47]H. R. Siekmann, E. Holub-Krappe, B. U. Wenger, Ch. Pettenkofer, and K. H. Meiwes-Broer, in *From Clusters to Crystals,* edited by P. Jena, S. N. Khanna, and B. K. Rao (Kluwer Academic, London, 1992), Vol. II, p. 1141.
[48]S. M. Foiles, M. I. Baskes, and M. S. Daw, Phys. Rev. B **33**, 7983 (1986).
[49]S. M. Foiles and M. S. Daw, Phys. Rev. B **38**, 12643 (1988).
[50]S. M. Foiles and J. B. Adams, Phys. Rev. B **40**, 5909 (1989).
[51]J. B. Adams, S. M. Foiles, and W. G. Wolfer, J. Mater. Res. **4**, 102 (1989).
[52]S. M. Foiles, Surf. Sci. **191**, L779 (1987).
[53]F. Willaime and C. Massobrio, Phys. Rev. B **43**, 11 653 (1991).
[54]J. S. Nelson, M. S. Daw, and E. C. Sowa, Phys. Rev. B **40**, 1465 (1989).
[55]R. Gaisch, J. K. Gimzewski, B. Reihl, R. R. Schlittler, M. Tschudy, and W. D. Schneider, Ultramicroscopy **42-44**, 1621 (1992).